Methods

Yukiko Tomooka*, Dominic Spothelfer, Anna Puiggali-Jou, Céline Tourbier, Esma Bahar Tankus, Florian M. Thieringer, Philippe C. Cattin, Georg Rauter and Manuela Eugster

Minimally invasive *in situ* bioprinting using tube-based material transfer

Minimal invasives *in-situ* Bioprinting mittels schlauchbasiertem Materialtransport

https://doi.org/10.1515/auto-2023-0060
Received April 15, 2023; accepted May 10, 2023

Abstract: Minimally invasive *in situ* bioprinting can potentially enhance the advantages of bioprinting, allowing the surrounding healthy tissue to be maximally preserved. However, the requirements for such a device are manifold and challenging to fulfill. We present an experimental bioprinting platform consisting of an extrusion system based on a tube mounted between an extrusion syringe and a dispensing nozzle. We investigated the influence of material transfer through a tube on the printing outcome. The results showed that it is feasible to form a continuous filament and print 3-dimensional structures using the developed platform.

Keywords: bioprinting; cartilage repair; *in situ*; minimally invasive.

Zusammenfassung: Minimalinvasives Bioprinting kann die Vorteile von Bioprinting verstärken, da das umliegende gesunde Gewebe bei minimalinvasiven Eingriffen weitestgehend erhalten bleibt. Die Anforderungen an ein minimalinvasives 3D-Druckgerät sind jedoch vielfältig und herausfordernd. Wir stellen eine experimentelle Bioprinting-Plattform vor, die es ermöglicht, die Herausforderungen von minimalinvasivem *in-situ*-Bioprinting zu bewältigen. Diese Plattform beinhaltet ein Extrusionssystem, welches eine Spritze über einen Schlauch mit einer Dosierdüse verbindet. Wir untersuchten den Einfluss des Materialtransfers durch den Schlauch auf das Druckergebnis. Die Ergebnisse zeigten, dass es möglich ist, mit der entwickelten Plattform ein Filament zu formen und 3-dimensionale Strukturen zu drucken.

Schlagwörter: Knorpelreparatur; Bioprinting; *in situ*; minimalinvasiv.

1 Introduction

Bioprinting technologies have rapidly advanced with the progress in biomaterial and printing technologies over the last decade [1]. Bioprinting is considered a form of three-dimensional (3D) printing that utilizes bio-inks to print 3D structures that mimic native tissues. Customized 3D structure implantation can be achieved by bioprinting, however, when pre-printed structures are implanted at a treatment site, there is a risk of contamination and disruption of the printed structure.

There has been a growing interest in *in situ* bioprinting in the last few years [2]. *In situ* bioprinting involves printing an uncured biomaterial directly into or onto the patient's body and curing the printed structure *in situ*. An improved conformability of printed structures with complex topographies and reduced risk of contamination during implantation are expected using *in situ* bioprinting.

Performing *in situ* bioprinting without exposing operational sites, i.e., minimally invasive bioprinting, has also been discussed [2, 3]. In general, the advantages of minimally invasive treatments include shorter recovery time, less damage, and less blood loss [4]. Keeping the surrounding tissue intact is particularly important for bioprinting

***Corresponding author: Yukiko Tomooka**, BIROMED-Lab, Department of Biomedical Engineering, University of Basel, Basel, Switzerland, E-mail: yukiko.tomooka@unibas.ch
Dominic Spothelfer, **Georg Rauter and Manuela Eugster**, BIROMED-Lab, Department of Biomedical Engineering, University of Basel, Basel, Switzerland, E-mail: dominic.spothelfer@unibas.ch (D. Spothelfer), georg.rauter@unibas.ch (G. Rauter), manuela.eugster@unibas.ch (M. Eugster)
Philippe C. Cattin, CIAN, Department of Biomedical Engineering, University of Basel, Basel, Switzerland, E-mail: philippe.cattin@unibas.ch
Anna Puiggali-Jou, Tissue Engineering and Biofabrication Lab, Department of Health Science and Technology, ETH Zürich, Zürich, Switzerland, E-mail: anna.puiggalijou@hest.ethz.ch
Céline Tourbier, **Esma Bahar Tankus and Florian M. Thieringer**, Swiss MAM Research Group, Department of Biomedical Engineering, University of Basel, Basel, Switzerland; and Clinic of Oral and Cranio-Maxillofacial Surgery, University Hospital Basel, Basel, Switzerland, E-mail: celine.tourbier@usb.ch (C. Tourbier), esma.tankus@unibas.ch (E.B. Tankus), florian.thieringer@usb.ch (F.M. Thieringer)

because creating living tissue and organs requires a delicate balance between the preservation of native tissue and the growth of new tissue. Furthermore, quick patient recovery times are critical in the context of bioprinting since the successful development and integration of the printed tissue or organ may depend on the patient's ability to recover and resume normal activities.

Despite the expected advantages of minimally invasive *in situ* bioprinting, there are various challenges that need to be tackled. These challenges are primarily attributed to the printing environment constraints: printing and curing inside the body in a limited workspace without causing damage to the surrounding tissue (e.g., thermal, chemical, or mechanical damage). Due to space limitations, miniaturization of the printing system is essential. In addition, options for biomaterials and curing methods are limited because biocompatibility has to be ensured. Furthermore, a system to monitor the printing process during a minimally invasive treatment is also required since the printing site cannot be directly observed (i.e., no direct line-of-sight).

Our ultimate goal is to develop a minimally invasive *in situ* bioprinting system based on our highly accurate parallel robot for minimally invasive laser osteotomy [5, 6] (Figure 1). We focus on articular cartilage repair inside the knee joint as our first target application. Cartilage is a central functioning element of the knee joint that supports body weight and reduces joint friction. However, the healing capacity of cartilage is very limited due to its low metabolism. Thus, damaged cartilage often requires surgical intervention. Depending on the treatment technique used, the treatment either repairs, replaces, or regenerates the cartilage [7].

Conventional techniques for cartilage repair include bone marrow stimulation, autologous chondrocyte implantation, and autologous osteochondral transplantation [8, 9]. Although successful in some aspects, each of these techniques has limitations. For instance, applicable defect size limitation [9, 10] or poor integration with the surrounding cartilage at the defect site [8, 9]. In addition, treatments that involve suturing of cartilage replacement grafts create new defects in healthy cartilage tissue.

Minimally invasive *in situ* bioprinting is a promising treatment option for cartilage repair. Cartilage is dependent on the diffusion of nutrients from the surrounding tissues and the movement of synovial fluid to meet its nutritional needs [11]. Thus, regular joint movement and dynamic load are important for maintaining a healthy articular cartilage metabolism. Minimally invasive *in situ* bioprinting can allow for better nutrient diffusion required for successful cartilage healing, and thus for fast patient recovery and fast return to normal activity.

We developed a bioprinting platform for cartilage repair to address the feasibility and challenges in a step-by-step manner. The developed bioprinting platform consisted of an extrusion system with a tube between an extrusion syringe and a dispensing nozzle (tube-based material transfer). In conventional bioprinters, materials are directly extruded from an extrusion syringe to a dispensing nozzle. The developed tube-based material transfer theoretically allows minimally invasive *in situ* bioprinting by inserting only an end-effector and a material transfer tube with a dispensing nozzle inside the body while space-consuming components (e.g., extrusion syringe) are placed outside the body. In addition, the tube-based material transfer allows using an endoscope-like slim and dexterous structure, which can provide access to a larger printing area in a confined space through a smaller incision.

In the study presented in this manuscript, we investigated the feasibility and challenges of bioprinting with tube-based material transfer. Specifically, the influence of printing parameters (i.e., temperature and diameters of material transfer tubes and dispensing nozzles) on filament formation at the dispensing nozzle was investigated. In addition, scaffold designs were printed to observe the fidelity and mechanical strength of the printed structures to be self-supporting over multiple layers.

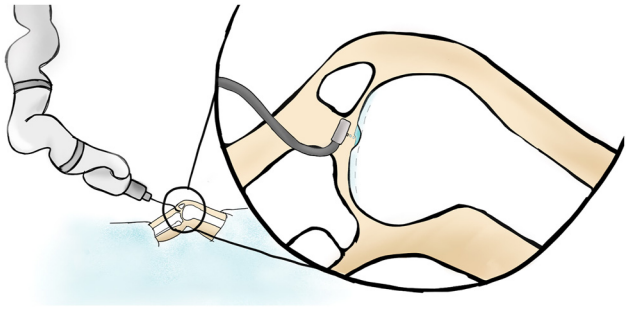

Figure 1: Conceptual drawing depicting minimally invasive *in situ* bioprinting for cartilage repair.

2 Technologies and state of the art in bioprinting

Current bioprinting mechanisms can be categorized into extrusion-based, inkjet-based, laser-based, and stereolithography-based bioprinting [12]. All four methods have their advantages and disadvantages [12] and a suitable mechanism needs to be selected depending on the application.

Appropriate material selection is essential to achieve desired clinical outcomes from bioprinting. Printability (e.g., appropriate viscosity range and mechanical strength), biocompatibility, mechanical properties, and biodegradability are important factors to consider when developing a biomaterial for bone or cartilage repair [13]. The three most common material categories for articular cartilage repair are synthetic polymers such as polylactic acid (PLA) or polycaprolactone (PCL), polysaccharide gels such as alginate, and protein-based materials such as gelatin [12].

A material curing process called cross-linking, which improves the mechanical, biological, and degradative properties of the printed material, is an important feature of bioprinting [14]. Cross-linking refers to inducing the formation of covalent or ionic bonds between polymer chains within a material to improve its properties [14, 15]. Various stimuli such as heat, pressure, change in potential hydrogen (pH), or light exposure can initiate cross-linking. In cartilage tissue engineering research, the material curing methods of choice are often photo-cross-linking and chemical cross-linking [3].

Major bioprinting research areas are biomaterial research, printing technology research, and application-driven research [1]. Typical bioprinting applications include printing bone tissue, vascular tissue, nervous system tissue, or cartilage tissue. Initially, bioprinting involved the design of porous structures used as scaffolding, which would ultimately absorb into the body and be replaced by native tissue. These techniques involved printing the porous structures in a controlled environment followed by implantation into the target region within the body. A significant amount of research has focused on bioprinting with post-printing implantation for cartilage repair [1], while only a few groups demonstrated *in situ* bioprinting for cartilage repair [16–18]. The presented *in situ* bioprinting systems in general utilized either hand-held or robotic approaches [3], including systems developed specifically for cartilage repair [16–18]. The main advantages of hand-held printing systems are portability and low cost of devices. On the other hand, robotic approaches have the advantage of higher dexterity in controlling the shape of printing structures in various printing environments, including minimally invasive environments.

Two groups reported minimally invasive *in situ* bioprinting systems for cartilage repair [19, 20]. Lenatowicz et al. showed a proof of concept of a minimally invasive *in situ* bioprinting approach for cartilage repair [20]. The proposed arthroscopic handheld 3D printing tool used a secondary tool holding a camera and an ultraviolet (UV) light source for monitoring and curing materials. Lipskas et al. developed a rigid endoscope-like robotic system with an extrusion mechanism to allow cartilage repair with minimally invasive bioprinting [19]. The performance of the developed robotic system was evaluated in an open space environment. To our best knowledge, research on performing *in situ* bioprinting for cartilage repair in a minimally invasive setting has not yet been published. In addition, both of the proposed systems were rigid devices, which may restrict access to a confined print site through a small incision.

Zhao et al. [21] and Thai et al. [22] developed flexible minimally invasive *in situ* bioprinting systems including tube-based material transfer for gastric wound treatments. The performances of the proposed systems were evaluated in minimally invasive *in vitro* settings. Although Zhao et al. discussed the necessity of preliminary printing parameter optimization, the influence of a material transfer tube and printing parameter selection (i.e., temperature and diameter of material transfer tube and dispensing nozzle) on filament formation was not elaborated in Zhao's work, or to our best knowledge, in any other published work.

3 Materials and methods

A printing material, printing mechanism, and cross-linking method that satisfy the requirements of minimally invasive *in situ* bioprinting were selected for the printing platform presented in this manuscript. Specifically, size constraints, temperature limitations, and minimal risk of surrounding tissue damage were considered as requirements for minimally invasive *in situ* bioprinting. The printing material was selected considering the targeted application (cartilage repair). For positioning a dispensing nozzle, a robotic approach was selected due to the greater dexterity in a confined workspace and higher accuracy in controlling the shape of printing structures compared to manual manipulation of hand-held tools. Precise shape control is essential for cartilage repair to allow smooth joint motion after a surgery. The extrusion-based bioprinting mechanism was selected because it allows the use of materials with a wide range of viscosities, thus providing various material options. The scaffold design, including filament diameter and pore size, is also important for successful tissue repair [23]. The nozzle sizes were selected considering the range of diameters found in literature attempting *in situ* cartilage repair [16, 18]. Gelatin methacryloyl (GelMa) was selected as a printing material due to its versatile material properties, including excellent biocompatibility, shear thinning property, and ability to fine-tune its viscosity through concentration and temperature [24]. Furthermore, the mechanical properties of printing material can be adjusted by regulating the GelMa concentration and UV dose [25, 26]. It has been shown that creating GelMa with a compressive modulus similar to that of native human articular cartilage is possible and GelMa has been successfully used for *in vitro* cartilage repair [25]. In addition, photoinitiated cross-linking was selected as our potential cross-kinking method due to the short cross-linking time and precise control over cross-linking density [27]. However, in the measurements performed in this study, no photoinitiator and no cross-linking process were included to eliminate the influence of unexpected cross-linking by environmental stimuli such as natural light on the measurement results.

3.1 Printing platform

The designed bioprinting platform consisted of (1) an end effector (Dexarm: Rotrics, Shenzhen, China), (2) an extrusion system, (3) an end-effector adaptor, (4) a proximity sensor (E2B-M12LS02-M1-B1: Omron Corporation, Kyoto, Japan), and (5) a printing bed made of an aluminum plate (Figure 2). The extrusion system, the end effector, and the printing bed were fixed to a rigid baseboard. The extrusion system consisted of (2.1) a pump (Hamilton Precision Syringe Drive: Hamilton Company, Nevada, United States) with an extrusion syringe, (2.2) a heating system on the extrusion syringe, (2.3) a dispensing nozzle, and (2.4) a polytetrafluoroethylene (PTFE) material transfer tube connecting the extrusion syringe to the dispensing nozzle.

The extrusion syringe was distally placed from the dispensing nozzle to enable minimally invasive bioprinting through a small incision. The dispensing nozzle and the proximity sensor for bed leveling were fixed to the end-effector adapter mounted on the end-effector. The heating system consisted of a temperature sensor (PT100: Thermokon Sensortechnik GmbH, Mittenaar, Germany) and an electric heating foil (Conflux AB, Jarfalla, Sweden). The heating system was fixed to the extrusion syringe with electrical tape to ensure it stayed in place and provided insulation of the material inside the syringe against ambient temperature. The developed bioprinting platform was controlled with a graphical user interface (GUI). For the control of the heating system as well as the reading of the signal from the proximity sensor, an Arduino Uno (Arduino, Turin, Italy) was utilized. The temperature sensor resistance value was translated to the respective temperature using a MAX31865 PT100 RTD temperature sensor amplifier (Adafruit Industries, New York, United States) and an Arduino library (Adafruit MAX31865, Adafruit Industries, New York, United States). The end effector was controlled using a Python script provided by the manufacturer (Rotrics, Shenzhen, China). The syringe pump was controlled using a modified Python library provided by the manufacturer (Hamilton Company, Nevada, United States).

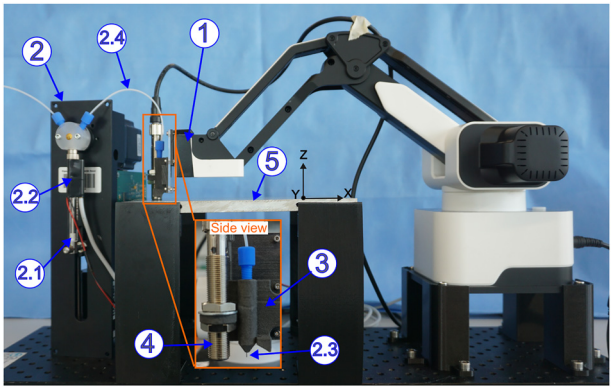

Figure 2: Bioprinting platform. (1) An end effector, (2) an extrusion system, (3) an end-effector adaptor, (4) a proximity sensor, and (5) a printing bed made of an aluminum plate. The extrusion system consisted of (2.1) a pump with an extrusion syringe, (2.2) a heating system on the extrusion syringe, (2.3) a dispensing nozzle, and (2.4) a polytetrafluoroethylene (PTFE) material transfer tube connecting the extrusion syringe and the dispensing nozzle.

3.2 Material synthesis

GelMa was synthesized from gelatin type A (from porcine skin, gel strength ≈300 g Bloom). An amount of 10 g gelatin type A was dissolved in 0.1 M carbonate-bicarbonate buffer (pH 9) and warmed up to 50 °C under vigorous stirring for 30 min. The total used methacrylic anhydride volume (1 mL) was split into five equal amounts (200 µL). For each portion, the pH of the solution was adjusted with sodium hydroxide and the solution was left to react for 30 min. After the last addition, the reaction was diluted twofold with distilled water and left to react for another 30 min. The product was cleaned by subsequent dialysis (10–12 kDa cutoff) against ultrapure water for four days. The solution was filtered, lyophilized, and stored at −20 °C until use. The lyophilized GelMa was diluted to ensure that the temperature at which the transition from a liquid state to a solid state (sol-gel transition) occurs is approximately the median of the temperature range achievable with the heating system (23 °C–40 °C). GelMa with an initial concentration of 20 % was synthesized according to the reconstitution protocol produced by CELLINK [28]. All GelMa concentrations were calculated as the weight of GelMa per total weight of GelMa and distilled water. Distilled water was used as a substitute for the phosphate-buffered saline (PBS) solution recommended in the protocol as it has a similar pH, which also contributes to the final viscosity pattern of the material. GelMa was mixed with the distilled water at 50 °C for 1 h each time the concentration was changed. GelMa was left to cool to room temperature and then reheated until the sol-gel transition was observed (30–40 °C). This process was iterated by adding additional volumes of distilled water until the sol-gel transition was observed at the desired temperature (30 °C). The final concentration of GelMa used for measurements was 8 %.

3.3 Printing parameter study

In the printing parameter study, we aimed to investigate the influence of temperature and the inner diameters of material transfer tubes and dispensing nozzles on filament formation at the dispensing nozzle. Specifically, we were interested in identifying at what temperature and with what dispensing nozzle inner diameter, the material can be extruded in a continuous filament form.

We performed measurements with four dispensing nozzle configurations, i.e., three tubes with different inner diameters $d_{i_N} = 0.25$ mm, 0.5 mm (both from Capillary tubing: VICI AG International, Luzerne, Switzerland), and 0.8 mm (PTFE tube: ROTIMA AG, Zurich, Switzerland) and a 23G needle ($d_{i_N} = 0.337$ mm) (AGAIM NEEDLE™: Terumo Corporation, Shibuya, Japan) at room temperature (23 °C). In the first three conditions, material transfer tubes of different inner diameters ($d_{i_T} = 0.25$ mm, 0.5 mm and 0.8 mm) connected the extrusion syringe to the end-effector adaptor, and the tips of the transfer tubes were directly used as dispensing nozzles ($d_{i_T} = d_{i_N}$). For the last condition, a material transfer tube ($d_{i_T} = 0.5$ mm) with a needle ($d_{i_N} = 0.337$ mm) mounted at the tip of the tube connected the extrusion syringe to the end-effector adaptor, and the needle was used as a dispensing nozzle. The inner diameters of the nozzles (d_{i_N}) and the wall thicknesses (t_N) of the dispensing nozzles, and the initial temperature at the extrusion syringe (T) used for the measurement are summarized in Table 1. The measurements were performed from top to bottom in the order shown in Table 1. The initial temperatures were selected to ensure a high enough temperature to observe the changes in the extruded material behavior from drops to filament. The material becomes more viscous as the nozzle's inner diameter decreases due to less material shear

Table 1: Dispensing nozzle sizes and initial temperatures at the extrusion syringe used for the printing parameter study.

Inner diameter d_{i_N}	Wall thickness t_N	Initial temperature T
0.25 mm	0.67 mm	36 °C
0.8 mm	0.395 mm	38 °C
0.5 mm	0.545 mm	32 °C
0.337 mm (23G)	0.152 mm	30 °C

thinning. Therefore, higher initial temperatures were required for the measurements using a nozzle with a larger inner diameter to allow observing drops. In all conditions, the extrusion syringe speed was fixed at its lowest setting of 2.5 steps/s, resulting in the material flow of 50 mm^3/min. The material transfer tubes had a length of 200 mm.

Each measurement consisted of the following procedure: the material was transferred into the extrusion syringe through manual drawing of the extrusion syringe drive. The material transfer tube was connected from the extrusion syringe to the end-effector adaptor. The extrusion syringe was heated continuously until the temperature of the extrusion syringe reached the defined initial temperature. The material was extruded at each initial extrusion syringe temperature. The extrusion syringe temperature was subsequently decreased by increments of 2 °C until printable material extrusion was observed at the dispensing nozzle outlet. Printable material extrusion refers to the extruded material forming a continuous filament. Non-printable material extrusion refers to no material extrusion, material dripping, or material forming a filament with an irregular diameter. During the extrusion, a series of photographs were taken to observe at which temperature the material was printable i.e., formed a continuous filament. Filament formation was observed from the visual inspection of the photographs. The extruded material was collected into a test tube and reused for subsequent measurements with different dispensing nozzle conditions.

3.4 3D structure printing test

After the printing parameter study, 3D structure printing tests with different scaffold designs were performed to study the fidelity of the scaffolds. The same material used for the printing parameter study was reused in the 3D structure printing test. The printing parameters used in the 3D structure printing tests are summarized in Table 2. The nozzle with inner diameter $d_{i_N} = 0.337$ mm was used for the 3D structure printing tests since it provided the thinnest continuous filament in the printing parameter study and, thus, the highest printing resolution. Two different density conditions of scaffolds were printed: 10 % and 30 % infill. Square single-layer scaffolds and 90° alternating two-layer scaffolds (20 mm × 20 mm) were printed for each density condition. The 3D structure printing tests were performed at room temperature (23 °C).

The scaffold designs were created using the CAD software Solidworks (Solidworks Corp., Massachusetts, United States) and the 3D printing slicer (Prusa Research, Prague, Czech Republic). Solid cubes designed by Solidworks were imported into the 3D printing slicer and the scaffold designs as well as the G-code was generated using the selected printing parameters summarized in Table 2. The layer thickness was set to 0.3 mm, which is thinner than the nozzle's inner diameter (i.e., 0.377 mm) to allow bonding between successive layers.

Table 2: Printing parameter values used for the 3D structure printing test.

Dispensing nozzle inner diameter d_{i_N}	0.337 mm
Material transfer tube length	200 mm
Material transfer tube inner diameter d_{i_T}	0.5 mm
Extrusion syringe temperature T	23 °C
Flow rate	50 mm^3/min
Print speed	9.34 mm/s

The position of the end effector in z-direction (Figure 2) was recorded at 16 positions on the print surface when the proximity sensor was triggered. The recorded position data for all 16 points were then used to calibrate the printing surface.

Each scaffold design was printed in the following procedure: the material was first transferred into the extrusion syringe through manual drawing of the extrusion syringe drive. The material transfer tube with the dispensing nozzle mounted at its tip connected the extrusion syringe to the end-effector adaptor. The extrusion syringe was heated to 23 °C. The material was printed onto the print surface by command of the user on a GUI and photographs of the printed structure were taken from the top to observe the fidelity and stability of the printed scaffolds. The printed scaffolds were observed based on visual inspection of the photographs.

3.5 Material degradation analysis

We analyzed the material degradation to examine whether the material degraded during the preceding printing parameter study since we reused the extruded material. After the printing parameter study had been completed, we selected a condition from the printing parameter study, where the continuous filament was formed properly (extrusion syringe temperature $T = 34$ °C, nozzle inner diameter $d_{i_N} = 0.8$ mm) and extruded the material once again. We checked whether a filament can be formed properly again. We inspected the extruded material visually.

4 Results

4.1 Printing parameter study

Photographs of extrusion using the dispensing nozzle with inner diameter $d_{i_N} = 0.5$ mm at varying extrusion syringe temperatures are shown in Figure 3. At 32 °C and 30 °C, a

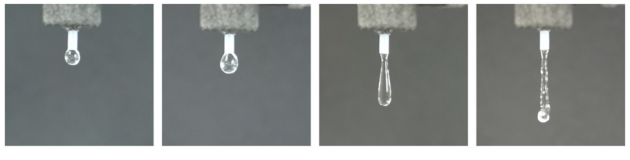

(a) $32°C$ **(b)** $30°C$ **(c)** $28°C$ **(d)** $26°C$

Figure 3: Extrusion of GelMa through tube of length 200 mm and nozzle inner diameter d_{i_N} of 0.5 mm. (a)–(b) Material instantly dripped, (c) material formed elongated drops, and (d) material formed an irregular filament.

dripping behavior of the extruded material was observed (Figure 3a and b). At 28 °C, the drops were elongated, however, the material dripped after a few millimeters of extrusion (Figure 3c). At 26 °C, the extruded material formed a filament and held its shape while being extruded, although having an irregular diameter (Figure 3d). The results of the printing parameter study are summarized in Figure 4 with example photos for each condition.

4.2 3D structure printing test

Photos of the different designs of printed scaffolds are shown in Figure 5. In double-layer prints, the second layer merged with the first layer in both 10 % and 30 % density conditions.

4.3 Material degradation analysis

We observed material dripping behavior at the dispensing nozzle at the condition at which a filament was successfully formed in the preceding printing parameter study (extrusion syringe temperature = 34 °C, dispensing nozzle inner diameter d_{i_N} = 0.8 mm), which indicated material degradation.

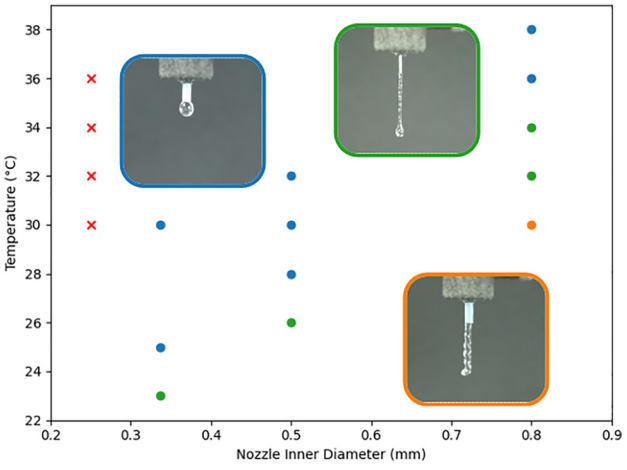

Figure 4: Printability of GelMa at different temperatures and nozzle inner diameters. The performed experiments are marked with crosses and dots. Red: no material extrusion, blue: dripping, green: filament formation, orange: irregular filament formation.

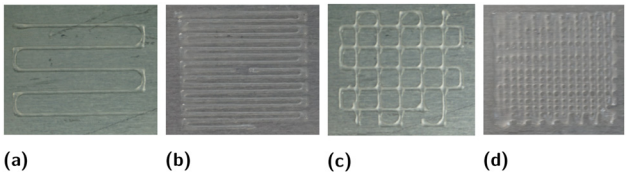

Figure 5: 3D printed scaffolds using GelMa with the dispensing nozzle inner diameter d_{i_N} = 0.337 mm and syringe temperature at 23 °C. (a) A single-layer print with 10 % infill, (b) a single-layer print with 30 % infill, (c) a double-layer print with 10 % infill, and (d) a double-layer print with 30 % infill.

5 Discussion

5.1 Printing parameter study

The results of the printing parameter study showed four distinct behaviors based on different combinations of temperature and nozzle inner diameter. The smallest nozzle d_{i_N} = 0.25 mm did not produce any extrusion out of the dispensing nozzle. We assume that the extrusion pump could not attain the required extrusion forces to push the material out of the small outlet, resulting in the dispensing nozzle being clogged. The material viscosity was not low enough to extrude for the smaller nozzle diameter. Lower material viscosity could be achieved using either a higher temperature or a GelMa with higher shear thinning properties.

Although filaments were formed with the larger dispensing nozzle inner diameters of d_{i_N} = 0.337 mm, 0.5 mm, and 0.8 mm, at specific temperatures, the extruded filaments exhibited irregularities in their diameter. This irregularity may have been caused by the discontinuous stepping behaviors of the stepper motor driving the syringe since the extrusion pump was operated at its lowest flow rate. The observed irregularities in filament diameter could be improved by using a dispensing unit that allows continuous syringe displacement at low flow rates.

The temperature at which the dispensing nozzle with inner diameter d_{i_N} = 0.5 mm formed a filament was almost 10 °C lower than that of the larger dispensing nozzle d_{i_N} = 0.8 mm. The temperature difference can be attributed to two factors. The first factor is the varied material viscosity due to shear thinning. Since all of the experiments were conducted with the same flow rate of 50 mm^3/min, the smaller the dispensing nozzle's inner diameter, the higher the material flow velocity in the dispensing nozzle, resulting in increased shear force and lower material viscosity. The second factor is the change in material temperature during its travel from the extrusion syringe to the dispensing nozzle through the material transfer tube. The thicker wall material transfer tube (d_{i_T} = 0.5 mm, t = 0.545 mm) insulated the material temperature more than the thin wall material transfer tube (d_{i_T} = 0.8 mm, t = 0.395 mm). Therefore, the thin wall material transfer tube is expected to have resulted in faster cooling of the material during the travel from the syringe outlet to the dispensing nozzle outlet, and therefore higher viscosity at the dispensing nozzle outlet. To minimize the surrounding environment's temperature

influence, controlling material temperature over the entire material path from the extrusion syringe to the dispensing nozzle exit would be ideal. Alternatively, a heating element could be installed near the dispensing nozzle to compensate for the material heat loss during transfer. Another option could be optimizing the material property considering the expected ambient temperature in the operating environment to minimize the influence of ambient temperature. Thus, biomaterials with wide adjustability in viscosity and shear thinning properties would be particularly beneficial for minimally invasive *in situ* bioprinting, where material temperature control is challenging.

We observed more material accumulation when the nozzle with the larger wall thickness ($d_{i_N} = 0.5$ mm, $t = 0.545$ mm) was used than when the nozzle with the smaller wall thickness was used ($d_{i_N} = 0.8$ mm, $t = 0.395$ mm). It is assumed that the wall thickness of the nozzle influences the material accumulation at the nozzle outlet due to the higher surface tension. The wall thickness of the dispensing nozzle should be minimized to alleviate the accumulation of material at the dispensing nozzle tip. Material dripping at the nozzle could be reduced by minimizing the material accumulation at the dispensing nozzle, leading to printable results over a wider range of material temperatures.

In this study, the influence of using varied extrusion pressure, induced by using different diameter tubes, on cell viability inside the material was not investigated. However, when cell-constituted biomaterial is involved, a method of measuring extrusion pressure should be incorporated into an extrusion pump since extrusion pressure control is essential to maintain a high cell viability rate. The temperature conditions tested in this study were close to human body temperature, thus, we assume that the temperature conditions we used would not diminish cell viability even when cell-constituting materials would be used.

5.2 Printing test

The designed scaffolds were successfully printed in two density conditions, 10 % and 30 % infill (Figure 5). Material accumulation was observed at sharp corners within the print. When attempting to print double-layer scaffolds, the first layer could not support the added material and the second layer merged with the first layer. This low stability was due to the low viscosity of the material and also because cross-linking was not performed. Further tuning of the material shear thinning property, the dispensing nozzle diameter, and the extrusion syringe temperature may allow continuous filament formation without clogging tubes while maintaining higher material viscosity after extrusion, resulting in higher stability of the printed structures.

Although the second layer merged with the first layer as expected, it was feasible to print continuous patterns in a setting where the material temperature could be controlled only at the extrusion syringe, which is placed at a distance of 200 mm from the dispensing nozzle (i.e., the length of the material transfer tube). However, in actual minimally invasive *in situ* bioprinting, a longer path from the extrusion syringe to the dispensing nozzle might be necessary. Thus, the influence of ambient temperature on the material temperature during the transfer is expected to be more significant.

The photoinitiator and the cross-linking procedure were not involved in this study. However, the cross-linking method and timing are expected to have a large effect on material behavior at the dispensing nozzle and printing outcome. Therefore, printing parameters and printing outcomes including cross-linking procedures should be investigated in the future to evaluate the feasibility of tube-based material transfer. Various timing of cross-linking during the printing process is applicable in bioprinting using photocrosslinking (i.e., cross-linking before, during, or after material deposition) [29, 30]. However, cross-linking before material deposition may be challenging in case of a tube-based material transfer since the tube may be clogged during material transfer. Furthermore, integrating a cross-linking mechanism into a robotic system for minimally invasive *in situ* bioprinting is also expected to add further challenges due to the limited space available to mount a cross-linking mechanism (miniaturization) and the risk of nozzle clogging during the cross-linking process.

5.3 Material degradation analysis

The performed material degradation analysis indicated that the viscosity of the material had decreased throughout the performed experiments. Since we reused the material in the printing parameter study and 3D structure printing test, the degradation of the material could have caused a decrease in viscosity over time. We assume that GelMA, being a hydrophilic material, absorbed moisture during the printing parameter study and 3D structure printing test. Moisture absorption could have decreased the material concentration and hence the viscosity. In order to mitigate material degradation in the future, it is suggested to use a fresh sample of material when conducting multiple experiments. Alternatively, the humidity of the experimental environment could be maintained low to avoid moisture absorption from the air.

Material degradation could have affected the printable temperature identified in the printing parameter study, specifically for the measurements with the nozzle inner

diameter $d_{i_N} = 0.5$ mm and $d_{i_N} = 0.337$ mm as they were tested last. If the material had not degraded during the printing parameter study, we would expect the printable region (green dots in Figure 4) at a higher temperature. Despite the degradation of the material, the results of the printing parameter study showed that continuous filament formation for varying nozzle inner diameters is possible by adjusting the extrusion syringe temperature with a bioprinting platform using tube-based material transfer.

The results obtained from the printing parameter study and printing test showed the feasibility of continuous filament generation and 3D structure printing using tube-based material transfer. Thus, the tube-based material transfer is an essential and promising element to deliver printing material to printing sites inside the patient's body in a minimally invasive manner. Our results showed that the material's temperature control is a key element to achieving consistent material extrusion, especially in the case of tube-based material transfer and under the influence of ambient temperature. The challenges of adding elements for temperature control and cross-linking to a miniaturized device will have to be overcome to realize minimally invasive *in situ* bioprinting in future.

6 Conclusions

We investigated the feasibility and challenges of bioprinting with a tube-based material transfer feasible for minimally invasive *in situ* bioprinting. Specifically, tube-based material transfer refers to a setup where the material is transferred to the dispensing nozzle through a tube connected to the extrusion syringe placed at a distance from the dispensing nozzle. We investigated the influence of printing temperature, material transfer tube diameter, and dispensing nozzle diameter on filament formation at the dispensing nozzle. We demonstrated that it is possible to achieve continuous filament formation for varying nozzle inner diameters by adjusting the extrusion syringe temperature. In addition, scaffold designs were printed to observe the fidelity and mechanical strength of the printed structures to be self-supporting over multiple layers. The designed scaffolds were successfully printed in two density conditions 10 % and 30 % infill, however, the first layer could not support the second layer and the second layer merged with the first layer for double-layer prints. Further fine-tuning of printing parameters (e.g., material viscosity and dispensing nozzle sizes) is required to improve the printed material's self-supporting ability.

The main challenges of using tube-based material transfer were the limited ability to control the material temperature at the dispensing nozzle and the influence of ambient temperature on material temperature, which both affected printing performance (filament formation). However, we consider tube-based material transfer as an essential element of minimally invasive *in situ* printing, the challenges it brings along seem to be controllable, allowing minimally invasive 3D bioprinting to become a treatment option.

Acknowledgment: The authors thank Prof. Dr. Marcy Zenobi-Wong for providing us with the biomaterials used in this work.

Author contributions: All the authors have accepted responsibility for the entire content of this submitted manuscript and approved submission.

Research funding: The authors gratefully acknowledge funding of the Werner Siemens Foundation through the MIRACLE project and Swiss Government Excellence Scholarship by Federal Commission for Scholarships for Foreign Students.

Conflict of interest statement: The authors declare no conflicts of interest regarding this article.

References

[1] S. Santoni, S. G. Gugliandolo, M. Sponchioni, D. Moscatelli, and B. M. Colosimo, "3D bioprinting: current status and trends—a guide to the literature and industrial practice," *Bio-Des. Manuf.*, vol. 5, pp. 14–42, 2022.

[2] A. MacAdam, E. Chaudry, C. D. McTiernan, D. Cortes, E. J. Suuronen, and E. I. Alarcon, "Development of in situ bioprinting: a mini review," *Front. Bioeng. Biotechnol.*, vol. 10, p. 940896, 2022.

[3] S. Singh, D. Choudhury, F. Yu, V. Mironov, and M. W. Naing, "In situ bioprinting – bioprinting from benchside to bedside?" Tech. Rep. improvements., 2020.

[4] F. Picard, A. Deakin, N. Balasubramanian, and A. Gregori, "Minimally invasive total knee replacement: techniques and results," *Eur. J. Orthop. Surg. Traumatol.*, vol. 28, no. 5, pp. 781–791, 2018.

[5] M. Eugster, J.-P. Merlet, N. Gerig, P. C. Cattin, and G. Rauter, "Miniature parallel robot with submillimeter positioning accuracy for minimally invasive laser osteotomy," *Robotica*, vol. 40, no. 4, pp. 1070–1097, 2022.

[6] M. Eugster, "Robotic system for accurate minimally invasive laser osteotomy," *Automatisierungstechnik*, vol. 70, no. 7, pp. 676–678, 2022.

[7] A. R. Memon and J. F. Quinlan, "Surgical treatment of articular cartilage defects in the knee: are we winning?" *Adv. Orthop.*, vol. 2012, p. 528423, 2012.

[8] S. H. Kim, D. Y. Park, and B.-H. Min, "A new era of cartilage repair using cell therapy and tissue engineering: turning current clinical limitations into new ideas," *Tissue Eng. Regen. Med.*, vol. 9, pp. 240–248, 2012.

[9] M. Tamaddon, L. Wang, Z. Liu, and C. Liu, "Osteochondral tissue repair in osteoarthritic joints: clinical challenges and opportunities

in tissue engineering," *Bio-Des. Manuf.*, vol. 1, pp. 101—114, 2018.
[10] A. M. Bhosale and J. B. Richardson, "Articular cartilage: structure, injuries and review of management," *Br. Med. Bull.*, vol. 87, pp. 77—95, 2008.
[11] A. J. S. Fox, A. Bedi, and S. A. Rodeo, "The basic science of articular cartilage," *Sports Health*, vol. 1, pp. 461—468, 2009.
[12] J. Huang, J. Xiong, D. Wang, et al., "3D bioprinting of hydrogels for cartilage tissue engineering," *Gels*, vol. 7, p. 144, 2021.
[13] N. Li, R. Guo, and Z. J. Zhang, "Bioink formulations for bone tissue regeneration," *Front. Bioeng. Biotechnol.*, vol. 9, p. 630488, 2021.
[14] J. Maitra and V. K. Shukla, "Cross-linking in hydrogels-a review," *Am. J. Polym. Sci.*, vol. 4, no. 2, pp. 25—31, 2014.
[15] A. D. Jenkins, P. Kratochvíl, R. F. T. Stepto, and U. W. Suter, "Glossary of basic terms in polymer science (IUPAC recommendations 1996)," *Pure Appl. Chem.*, vol. 68, pp. 2287—2311, 1996.
[16] K. Ma, T. Zhao, L. Yang, et al., "Application of robotic-assisted in situ 3D printing in cartilage regeneration with HAMA hydrogel: an in vivo study," *J. Adv. Res.*, vol. 23, pp. 123—132, 2020.
[17] C. Di Bella, S. Duchi, C. D. O'Connell, et al., "In situ handheld three-dimensional bioprinting for cartilage regeneration," *J. Tissue Eng. Regen. Med.*, vol. 12, no. 3, pp. 611—621, 2018.
[18] B. Gatenholm, C. Lindahl, M. Brittberg, and S. Simonsson, "Collagen 2A type B induction after 3D bioprinting chondrocytes in situ into osteoarthritic chondral tibial lesion," *Cartilage*, vol. 13, pp. 1755S—1769S, 2021.
[19] J. Lipskas, K. Deep, and W. Yao, "Robotic-assisted 3D bio-printing for repairing bone and cartilage defects through a minimally invasive approach," *Sci. Rep.*, vol. 9, no. 1, pp. 1—9, 2019.
[20] K. Lenartowicz, T. Gapiński, P. Galas, M. Gonsior, L. Ricotti, and L. Vannozzi, "3D bioprinting handheld tool concept for innovative osteoarthritis treatment with stem cells utilization," *Eng. Biomater.*, vol. 22, no. 153, p. 44, 2019.
[21] W. Zhao and T. Xu, "Preliminary engineering for in situ in vivo bioprinting: a novel micro bioprinting platform for in situ in vivo bioprinting at a gastric wound site," *Biofabrication*, vol. 12, p. 045020, 2020.
[22] M. T. Thai, P. T. Phan, H. A. Tran, et al., "Advanced soft robotic system for in situ 3d bioprinting and endoscopic surgery," *Adv. Sci.*, vol. 10, p. 2205656, 2023.
[23] L. Belk, N. Tellisi, H. Macdonald, A. Erdem, N. Ashammakhi, and I. Pountos, "Safety considerations in 3D bioprinting using mesenchymal stromal cells," *Front. Bioeng. Biotechnol.*, vol. 8, p. 924, 2020.
[24] Y. Piao, H. You, T. Xu, et al., "Biomedical applications of gelatin methacryloyl hydrogels," *Eng. Regen.*, vol. 2, pp. 47—56, 2021.
[25] J. Liu, L. Li, H. Suo, M. Yan, J. Yin, and J. Fu, "3D printing of biomimetic multi-layered GelMA/nHA scaffold for osteochondral defect repair," *Mater. Des.*, vol. 171, p. 107708, 2019.
[26] W. Schuurman, P. A. Levett, M. W. Pot, et al., "Gelatin-methacrylamide hydrogels as potential biomaterials for fabrication of tissue-engineered cartilage constructs," *Macromol. Biosci.*, vol. 13, no. 5, pp. 551—561, 2013.
[27] G. S. Krishnakumar, S. Sampath, S. Muthusamy, and M. A. John, "Importance of crosslinking strategies in designing smart biomaterials for bone tissue engineering: a systematic review," *Mater. Sci. Eng. C*, vol. 96, pp. 941—954, 2019.
[28] CELLINK, *Reconstitution-protocols-photogel-50-ds 8-feb-2023*, Available at: https://www.cellink.com/wp-content/uploads/2023/02/Reconstitution-Protocols-PhotoGel-50-DS_8-Feb-2023.pdf, Version 6 [accessed: Mar. 12, 2023].
[29] E. Mueller, I. Poulin, W. J. Bodnaryk, and T. Hoare, "Click chemistry hydrogels for extrusion bioprinting: progress, challenges, and opportunities," *Biomacromolecules*, vol. 23, pp. 619—640, 2022.
[30] L. Ouyang, C. B. Highley, W. Sun, and J. A. Burdick, "A generalizable strategy for the 3D bioprinting of hydrogels from nonviscous photo-crosslinkable inks," *Adv. Mater.*, vol. 29, no. 8, p. 1604983, 2017.

Bionotes

Yukiko Tomooka
BIROMED-Lab, Department of Biomedical Engineering, University of Basel, Basel, Switzerland
yukiko.tomooka@unibas.ch

Yukiko Tomooka obtained her Master's degree in Mechanical Engineering. She is pursuing her Ph.D. studies at BIROMED-Lab under the supervision of Prof. Dr. Georg Rauter at the University of Basel. Her research interest includes the development of mechanical and robotic systems for biomedical applications.

Dominic Spothelfer
BIROMED-Lab, Department of Biomedical Engineering, University of Basel, Basel, Switzerland
dominic.spothelfer@unibas.ch

Dominic Spothelfer obtained a BE in Mechanical Engineering at McGill University in 2018 and is currently pursuing a master's degree in Robotics, Systems, and Control at ETH Zurich. He conducted his master's thesis project at the BIROMED-Lab at the University of Basel. His interests lie in advancing medical technologies using robotic devices.

Anna Puiggalí-Jou
Tissue Engineering and Biofabrication Lab, Department of Health Science and Technology, ETH Zürich, Zürich, Switzerland
anna.puiggalijou@hest.ethz.ch

Anna Puiggalí obtained her BSc in Biochemistry from the Universitat de Barcelona in 2013, followed by an MSc in Biomedical Research from the Universitat Pompeu i Fabra in 2014. In March 2019, she earned her PhD in Biomedical Engineering from the Universitat Politècnica de Catalunya. Following that, she won an iMSCA fellowship and relocated to ETH Zurich.

Céline Tourbier
Swiss MAM Research Group, Department of Biomedical Engineering, University of Basel, Basel, Switzerland; and Clinic of Oral and Cranio-Maxillofacial Surgery, University Hospital Basel, Basel, Switzerland
celine.tourbier@usb.ch

Céline Tourbier is a dentist and aspiring CMF surgeon completing her second medical degree at Albert-Ludwigs University, Freiburg. As a researcher at the University Hospital Basel and the Department of Biomedical Engineering at the University of Basel, she is working on advancing 3D printing for bone regeneration in CMF surgery.

Esma Bahar Tankus
Swiss MAM Research Group, Department of Biomedical Engineering, University of Basel, Basel, Switzerland; and Clinic of Oral and Cranio-Maxillofacial Surgery, University Hospital Basel, Basel, Switzerland
esma.tankus@unibas.ch

Esma Bahar Tankus obtained her Master's degree in Medicine and diploma as a federal doctor from the University of Bern in 2022. Currently, she is pursuing her PhD in osteochondral tissue regeneration using 3D bioprinting, under Prof. Florian Thieringer and Prof. Andrea Barbero at the Swiss MAM and Cartilage Engineering groups.

Florian M. Thieringer
Swiss MAM Research Group, Department of Biomedical Engineering, University of Basel, Basel, Switzerland; and Clinic of Oral and Cranio-Maxillofacial Surgery, University Hospital Basel, Basel, Switzerland
florian.thieringer@usb.ch

Florian M. Thieringer, MD, DDS, MHBA, chairs Oral & Cranio-Maxillofacial Surgery at the Univ. Hospital Basel. He leads Swiss MAM at the Dept. of Biomed. Engineering, Unibas. Co-PI of MIRACLE II, revolutionizing bone surgery via robotic endoscopes, & patient-tailored implants.

Philippe Cattin
CIAN, Department of Biomedical Engineering, University of Basel, Basel, Switzerland
georg.rauter@unibas.ch

Philippe Cattin is a Swiss Professor of Biomedical Engineering at the University of Basel, and head of the Department of Biomedical Engineering. His research interests include medical image analysis, image-guided therapy, and virtual reality. He has published more than 250 papers, patents, and book chapters, and founded three spin-off companies.

Georg Rauter
BIROMED-Lab, Department of Biomedical Engineering, University of Basel, Basel, Switzerland
manuela.eugster@unibas.ch

Georg Rauter is Associate Prof. for Surgical Robotics at the BIROMED-Lab. His background is Mechanical Engineering (TU-Graz) and Mathematical and Mechanical Modeling (MATMECA, Bordeaux). In 2014 he received his PhD in robotics from ETH Zurich.

Manuela Eugster
BIROMED-Lab, Department of Biomedical Engineering, University of Basel, Basel, Switzerland
philippe.cattin@unibas.ch

Manuela Eugster works since 2016 as a researcher at the BIROMED-Lab. She has a Master's Degree in Mechanical Engineering (ETH Zurich) and a PhD in Biomedical Engineering (University of Basel). Her main research focus is the design of complete robotic and mechatronic systems for biomedical applications.